FISEVIER

Contents lists available at ScienceDirect

Polymer Testing

journal homepage: http://www.elsevier.com/locate/polytest





Synthesis of microwave-mediated biochar-hydrogel composites for enhanced water absorbency and nitrogen release

Yudi Wu^a, Colten Brickler^a, Simeng Li^{b,*}, Gang Chen^a

- a Department of Civil and Environmental Engineering, FAMU-FSU College of Engineering, 2525 Pottsdamer Street, Tallahassee, FL, 32310, United States
- b Department of Civil Engineering, California State Polytechnic University Pomona, 3801 West Temple Avenue, Pomona, CA, 91768, United States

ARTICLE INFO

Keywords:
Biochar
Microwave irradiation
Nitrogen release
Soil amendment
Superabsorbent hydrogel
Water absorbency

ABSTRACT

Superabsorbent hydrogels have been used to enhance water and nutrient retention in agricultural soils. However, wide applications of these polymeric soil amendments on large farms are plagued by their high costs and environmental footprints. Therefore, solutions are urgently needed in order to optimize the hydrogel application. Biochar, which is a cost-effective pyrolysis product, has been applied as soil amendments for soil fertility reservation. In this study, biochar was co-polymerized with hydrogels to explore the agronomic potentials. Biochar-hydrogel composites were synthesized through rapid mediation of microwave radiation. The physicochemical properties of these composites, such as surface functionality, thermal stability, and morphology, were characterized using various state-of-the-art analytical techniques. The discoveries in this study demonstrated that microwave irradiation could effectively facilitate structural alteration and optimize cross-linkage of biocharhydrogel composites. Biochar-hydrogel composite (7.5% w/w biochar/composite) significantly improved swelling capacity (20.18% water was absorbed after 48 h) and optimized the nitrogen release (20.03% of nitrogen was release after 30 days) of composites. Water adsorption and nitrogen release obeyed Gallagher-Corrigan model and Korsmeyer-Peppas model, respectively. The results revealed the microwave-irradiated biochar-hydrogel composite is a promising soil amendment with regard to economic benefit and environmental footprint.

1. Introduction

Excessive irrigation and inefficiency of instant fertilizer are two major issues last for a very long time in agricultural practices [1]. It was estimated that 40%–60% of irrigation water has been leached through subsurface soil and erosion [2]. At the same time, agricultural fertilizers contribute significant amounts of phosphorus (P) and nitrogen (N) fluxes to lakes and rivers in the United States because of wasteful water usage. 70% of N and P input to the Gulf of Mexico, where dead zone and eutrophication kept recurring, came from the agricultural activity of the upper river basin [3]. Therefore, it is an exigency to solve these two major concerns (i.e., excessive irrigation and inefficiency of instant fertilizer) to enhance the agricultural production.

Efforts have been made on the enhancement of instant fertilizer efficiency. Enhanced efficiency fertilizers (EEFs) are proposed to control fertilizer release or eliminate reactions that lead to nutrient losses. Different EEFs such as sulfur-coated urea, polymer-coated urea, and urea formaldehyde were widely investigated in previous studies. The

application of attapulgite-coated fertilizer successfully increased the maize yield by 15%-18% [4]; polymer-coated urea was able to enhance the grain yield to 26.4% [5]. However, the performances of EEFs are largely dependent on the geographical conditions and climate. Although N₂O emission showed a significant decrease on the site applying polymer-coated urea, the crop yield and nitrogen usage efficiency were not affected in tropical cropping system [6]. Targeting on balancing the inconsistency of EEFs' performance, biochar is proposed to be co-applied with EEFs. Because of its multi-benefits and cost effectiveness, biochar has been assigned extensively in agriculture and horticulture for enhancements of soil fertility, crop production, water storage and microorganism activity in soil environments [7]. It has been observed that up to 70% increase in crop yield could be achieved in nutrient-poor tropical soil with addition of nutrient biochar [8]. At the same time, soil microbes exhibited strengthened resistance and resilient to the drought after applying biochar, which would be helpful for the nutrient cycling and soil carbon sequestration simultaneously [9]. Moreover, the introduction of biochar enhances the mechanical strength

E-mail address: sli@cpp.edu (S. Li).

^{*} Corresponding author.

and prolong the nutrient release period, demonstrating great potential for improving performance of EEFs [10].

Hydrogel is suitable to be a coating material as it provides protection to stored nutrients from leaching as well as store appreciate amount of water. Hydrogels are crosslinked polymers, on which hydrophilic functional groups are attached [11]. Their distinct permeable structures and diverse hydrophilic functional groups make them potential reservoirs for excess water and nutrients in agricultural soils. A prior review reported that conventional polyacrylamide hydrogels could retain distilled water of as much as 326 times their dry weight [12]. Despite its promising application to EFFs, the major issue of this novel technology is its weak biodegradability. Conventional hydrogels such as polyacrylic acid and polyacrylamide are difficult to decompose, which consequently leads to the undesirable environmental footprint [13]. Cellulose, which is an abundant natural polymer, is considered for eliminating the disadvantages of conventional polymers [14].

The major concerns of a classical polymerization of hydrogel are the involvement of organic solvents and production of byproducts [15]. Conventional heating during polymerization employs long-period rotations in an organic media. Hydrogels derived from classical methods retain additives and residues, which pose severe environmental threats if directly be applied into the agricultural field [16]. The removal of byproducts requires high temperature and high vacuum [17]. Hence, microwave-mediated polymerization, which is clear from the organic solvents and byproducts, is promising for green production. Microwave irradiation provides rapid dipole rotation and generate inherent heat within the materials, which significantly speed up the reaction process and limit the side reactions [18]. Giachi et al. demonstrated that a microwave-irradiated hydrogel exhibited a faster swelling and shrinking behavior [19]. High efficiency of microwave irradiated cellulose/acrylamide hydrogel for delivering oral drug was also demonstrated, with the properties of non-cytotoxicity and biocompatibility [20]. Although the major advantages of microwave irradiation are high efficiency of polymerization and cleaner process, it is significant to estimate its cost-effectiveness. Because of its simple apparatus, limited additives, and easy control, it can largely reduce processing cost and labor cost. However, few studies have reported biochar-hydrogel composites via microwave irradiation that can retain water and release nutrients.

The main objective of this study is to propose an efficient and cost-effective biochar-hydrogel composite using microwave-irradiated polymerization. It is hypothesized that microwave irradiation is an efficient strategy for polymerization. And the biochar-hydrogel composites would exhibit great water retention and nitrogen release. Biochar in the biochar-hydrogel composite is expected to prolong nitrogen release period and retain larger amount of water than the composite without biochar. At the same time, different dosages of biochar would alter the structure architecture of the composite. To evince the structural characterizations and morphology of synthesized composites, thermogravimetric (TG) analysis, Fourier transform infrared spectroscopy (FTIR), and scanning electron microscope (SEM) would be utilized. Water retention and nitrogen release behavior were also analyzed.

2. Materials and methods

2.1. Slow pyrolysis of biochar synthesis

Biochar was produced from switchgrass (*Panicum virgatum*). Switchgrass (SG) is a perennial lowland species, which is prevalent in Florida. The original SG feedstock was dried at 60 °C for 48 h until no significant weight change was observed. Biochar was synthesized through slow pyrolysis. During the pyrolysis, pure N_2 gas (purity >99.99%) was used at temperatures 500 °C in a bench scale pyrolysis apparatus described in previous study [21]. In brief, dried feedstock (between 10 and 14 g) was centered in a quartz tube (inner diameter: 2 cm, length: 45 cm). The tube was fitted with airtight connectors and rubber O-rings. The tube packed with feedstock was heated in a

controllable S-line single-zone split tube furnace (Thermcraft Inc., Wiston-Salem, NC) at heat ramp of 10 $^{\circ}$ C min $^{-1}$ until the desired temperature and was kept at designate temperature for 60 min. The quartz tube was purged with N $_2$ gas (80 mL min $^{-1}$) during pyrolysis and cooling to prevent rapid oxidation and/or auto-ignition.

2.2. Preparation of biochar-hydrogel composite

Acrylamide (MAA, purity >99.99%), cellulose, urea fertilizer, potassium persulfate (KPS, purity >99%), N, N'-methylene bisacrylamide (MBA, purity: 99%) were purchased from Sigma—Aldrich (Steinheim, Germany). Materials were ground using a pestle and mortar, sieved to be less than 0.5 mm in diameter. A Domestic Electric microwave (JES2051SNSS, General Electric, Boston, MA), which possesses a 2.45 GHz frequency and a maximum 1650 W power output was utilized for the synthesis of biochar-hydrogel composites. Each sample solution containing 0.3 g of urea, 0.4 g of cellulose, 3 g MAA, 0.03 g KPS, 0.03 g MBA and 40 mL distilled water was introduced to a 100 mL glass container. Four samples containing biochar dosages of 0 g, 0.1 g, 0.2 g and 0.3 g are named as composite 1, 2, 3, and 4, respectively. Therefore, biochar constituted approximately 0%, 2.5%, 5.0%, and 7.5% (w/w) of four composites. The mixed solutions have been stirred until homogeneity and then flushed with N₂ gas for 20 min. Two power levels, Level 3 (495 W) and Level 5 (825 W), were used to synthesize. The samples were irradiated for 1 min at the two power levels, respectively. The products were washed with distilled water and dried to constant weight in an oven at 60 °C for further use.

2.3. Physicochemical properties characterization of biochar and biocharhydrogel composite

2.3.1. Fourier transform infrared spectroscopy (FTIR) analysis

FTIR spectra of raw materials (i.e., urea, cellulose, MAA and SG biochar) and biochar-hydrogel composites were recorded on a PerkinElmer 100 spectrometer (Waltham, MA) using non-contact reflectance imaging method. Raw materials and composites were ground to fine particles using a pestle and mortar. The FTIR spectra were conducted in the region of 4000 to 650 ${\rm cm}^{-1}$ with a spectral resolution of 4 ${\rm cm}^{-1}$ and total number of 16 scans per sample. Before each measurement, background spectrum was scanned without loading samples for calibration.

2.3.2. Thermogravimetric analysis (TGA)

Thermal behavior of raw materials (i.e., urea, cellulose, MAA and SG biochar) and biochar-hydrogel composites were analyzed using an MS-TGA thermogravimetric analyzer (GA 550, TA Instrument, New Castle, DE) under a flow of argon (50 mL min $^{-1}$) Each time, 5 mg of sample was weighed and then used for the thermal weight-change analysis. The temperature ramp was set as follows: (1) isotherm at room temperature (21 $^{\circ}$ C) for 5 min; (2) temperature equilibrium at 21 $^{\circ}$ C-100 $^{\circ}$ C; (3) isotherm at (100 $^{\circ}$ C) for 5 min; (4) ramping of 5 $^{\circ}$ C min $^{-1}$ from 100 $^{\circ}$ C to 700 $^{\circ}$ C.

2.3.3. Morphology analysis

The surface morphology of four different biochar-hydrogel composites and SG biochar were investigated via a FEI Nova 400 Nano SEM (Hillsboro, OR). Samples were first coated with iridium (Ir) via sputter coater (Cressington HR208 Sputter Coater, Ted Pella, Inc) with N_2 gas purging to dissipate charging artifacts and minimize the beam damage. As a result, a 4 nm coat was applied to each sample. Images were taken on samples under vacuum environment following the standard procedures at scales ranging from 2 to 50 μm . Characterization of surface morphology was performed using the SEM detector (Energy Dispersive Spectroscopy, ETD) at voltage between 10 and 20 kV, current of 96 pA, and focal length between 5 mm and 10 mm.

2.4. Study of water absorbency and fertilizer release properties of biochar-hydrogel composite

2.4.1. Measurements of water absorbency capacity and nutrient release

Water absorbency of biochar-hydrogel composites were examined using a gravimetric method. Weighted dry sample (1.0 \pm 0.1 g) was immersed in 50 ml distilled water at room temperature and allowed to reach equilibrium water absorbency. In order to determine the sorption kinetics, tests were run where at designated intervals. The water absorption capacity f_1 is calculated using the following equation:

$$f_1 = (M_t - M_1) / M_1 \times 100\% \tag{1}$$

Where M_t (g) is the weight of sample after water absorbency, M_1 (g) is the weight of dry sample at initial stage.

Nitrogen release profile f_2 of biochar-hydrogel composite were measured by a batch-scaled experiment. Weighted dry sample (1.0 \pm 0.1 g) was incubated in a glass bottle of 20 mL distilled water. 20 mL sample were taken at designated intervals and fresh distilled water was added immediately to keep the volume constant. The accumulated release of urea fertilizer was measured in form of total nitrogen in the solution following a persulfate digestion method. The absorbance of sample solution was then detected by a visible spectrophotometer (DR 3900, Hach, Loveland, CO) to quantify total nitrogen concentration. The amount of released nitrogen is calculated using the following equation:

$$f_2 = (C_2 \times V_2 - C_1 \times V_1) / M_3 \times 100\%$$
 (2)

Where M_3 (g) is the initial weight of urea fertilizer (in form of nitrogen) in the composite, V_1 (L) is the initial volume of sample solution in the glass bottle, C_1 (mg L^{-1}) is the initial nitrogen concentration in the glass bottle. C_2 (mg L^{-1}) is the nitrogen concentration in the sample solution, V_2 (L) is the volume of sample. The measurements of water absorbency and nitrogen release was tripled for each sample, respectively.

2.4.2. Water absorbency kinetics

The absorbency characteristic has been described as a quick swelling burst and then followed by a slower absorbency. To better understand the absorbency mechanism, the Gallagher-Corrigan model was applied to describe the data. Gallagher-Corrigan model divides the water absorbency profile into two stages, i.e., biphasic water absorbency consisting of a first-order quick burst and a subsequent smooth diffusion controlled by polymer degradation [22]. The quick burst and smooth diffusion are denoted as Stage I and Stage II, respectively.

$$(0.5 < n < 1.0)$$
 [23].

2.5. Statistical analysis

The experimental data were processed and analyzed by one-way analysis of variance (ANOVA) using SPSS for Windows 14.0 (IBM, Armonk, NY). The corresponding Scheffé test was made to differentiate means with 95% confidence (p < 0.05) when the study of variance showed differences between means.

3. Results and discussion

3.1. Surface structure analysis of biochar-hydrogel composite

Intermolecular interactions affect the vibration of groups on polymer segments. This information can be obtained by FTIR analysis (Fig. 1). In general, composites with higher dosages of biochar resulted in low transmission, which indicates enhanced molecular vibrations and/or complexity of structure. Aromatic and heteroaromatic compounds on SG biochar are confirmed by C-H wagging vibrations between 800 and 700 cm⁻¹. In the same region, the spectrum of composite 1 to composite 4 revealed peaks with different transmittances. Higher absorbency exhibited on the composite 4 spectrum, which might result from the increasing dosage of biochar. The spectrum of cellulose, MAA and biochar showed multiple peaks in the region of $990-1215 \, \mathrm{cm}^{-1}$. The C–O–C stretching of cellulose, hemicellulose, and lignin is the reason of observed peaks on cellulose spectrum and biochar spectrum. This base region overlapped the bands of Si-O (1030-950 cm⁻¹) observed on biochar [21]. Silica is the essential element for plant phytoliths, as it could protect the plant carbon from degradation. On MAA spectrum, the peaks in this region are usually assigned to the C-N-H stretching [24]. Therefore, the nadir in the region of 990–1215 cm⁻¹ on the composite spectrums might have several contributions: 1) C-O-C stretching on cellulose and biochar surface; 2) Si-O bands on biochar surface; 3) the linkage of crosslinked MAA and cellulose. Similar results have also revealed in previous studies, such as chitosan/biochar hydrogel [25] and carboxymethyl cellulose-acrylamide-graphene oxide composite [26]. The peaks at 1460 and 1662 cm⁻¹ on composite spectrums indicated the characteristic absorption of amine C-NH bond and CH2-CO-NH bending vibration, combinedly corresponding to the urea and MAA structure [27]. The absorption peaks at 2910, 3183, and 3330 \mbox{cm}^{-1} ascribes to C–H and O–H stretching vibration. The band at 3330 cm⁻¹ might also be attributed to the overlapping vibration of O-H and

$$f_1 = (f_1)_B \left[1 - exp(-k_{g,1} \times t) \right] + \left[(f_1)_{max} - (f_1)_B \right] \left[exp(k_{g,2} \times t - k_{g,2} \times t_{max}) / \left(1 + exp(k_{g,2} \times t - k_{g,2} \times t_{max}) \right) \right]$$
(3)

where, $(f_1)_B$ is the cumulative absorbency profile in Stage I; $K_{g,1}$ and $K_{g,2}$ are the absorbency factors in Stage I and Stage II, respectively; and $(f_1)_{max}$ is the maximum absorbency ratio during the process.

2.4.3. Nutrient release kinetics

Korsmeyer-Peppas model has been applied to study the mechanism of nutrients release. The release mechanism can be explained by the combined effect of polymer matrix relaxation and concentration-dependent diffusion [5].

$$f2 = K_K t^n (4)$$

where K_K and n swelling rate constant in the Korsmeyer-Peppas model and diffusion exponent, respectively. The exponent n in the equation indicates different swelling behaviors: 1) Fickian/case I transport (n=0.5); 2) n=1.0, case II transport (n=1.0); and 3) anomalous transport

N-H stretching [28].

3.2. Thermogravimetric characteristics of biochar-hydrogel composites

TG and DTG decomposition curves were analyzed for thermal stability. The composites exhibited three distinct stages of decomposition from 50 to 700 °C. Initially, the thermal peaks observed before 100 °C are contributed to the moisture loss associated with the hydrogel and biochar (Fig. 2 (d)) [21]. These thermal peaks increased with the increasing dosage of biochar. This might indicate that biochar helped preserve water in the composite. The second stage between 200 and 300 °C can be interpreted as the result of labile functional groups on MAA and cellulose, leading to the ammonia, CO and CO₂ formation (Fig. 2 (e)) [29]. Temperature at which maximum decomposition rate occur, i.e., T_{max} is found within the temperature from 360.31 to 382.44 °C. The last stage of degradation and T_{max} can be ascribed to

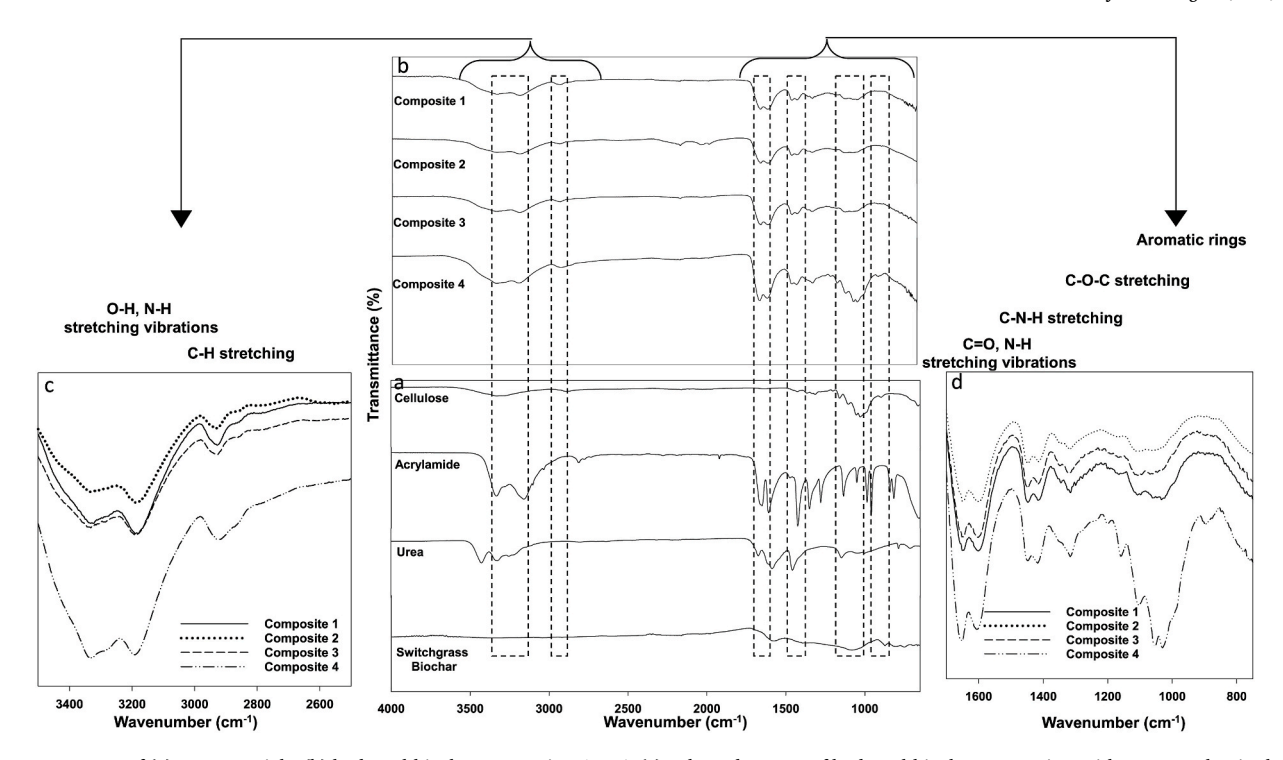


Fig. 1. FTIR spectra of (a) raw materials; (b) hydrogel-biochar composites 1 to 4; (c) enlarged spectra of hydrogel-biochar composites with wavenumber in the range of 3500 to 2500 cm⁻¹ and (d) enlarged spectra of hydrogel-biochar composites with wavenumber in the range of 1700 to 680 cm⁻¹.

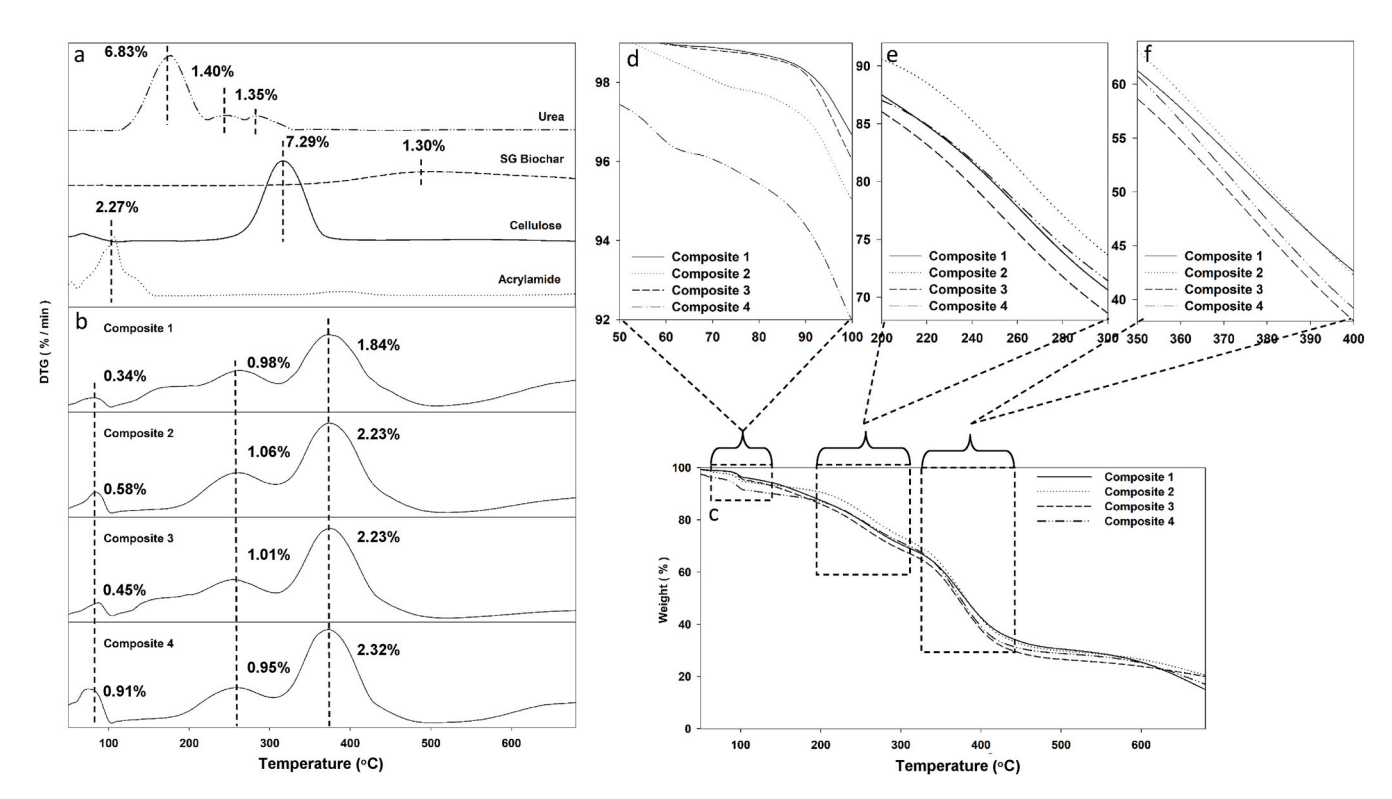


Fig. 2. (a) DTG curves of raw materials; (b) DTG curves of hydrogel-biochar composites 1 to 4; (c) TG curve of hydrogel-biochar composites 1 to 4; (d) to (f) are enlarged TG curves of hydrogel-biochar composites 1 to 4 with temperature in range of 50–100, 200 to 300 and 350 to 400, respectively.

main-chain scission and the destruction of crosslinked matrix (Fig. 2 (e)) [30]. Four composites exhibited parallel rates of destruction. T_{max} (360.31–382.44 °C) of four composites was clearly higher than that of the raw materials (Fig. 2 (a) and Fig. 2 (b)). Different dosages of biochar in samples did not alter the thermal stability. Microwave irradiation

efficiently produced the crosslinking characteristic, resulting a stabilized composite than the raw materials. This conclusion is consistent with previous study, which reported the crosslinking of cellulose and gelatin is responsible for the improved thermal stability [31].

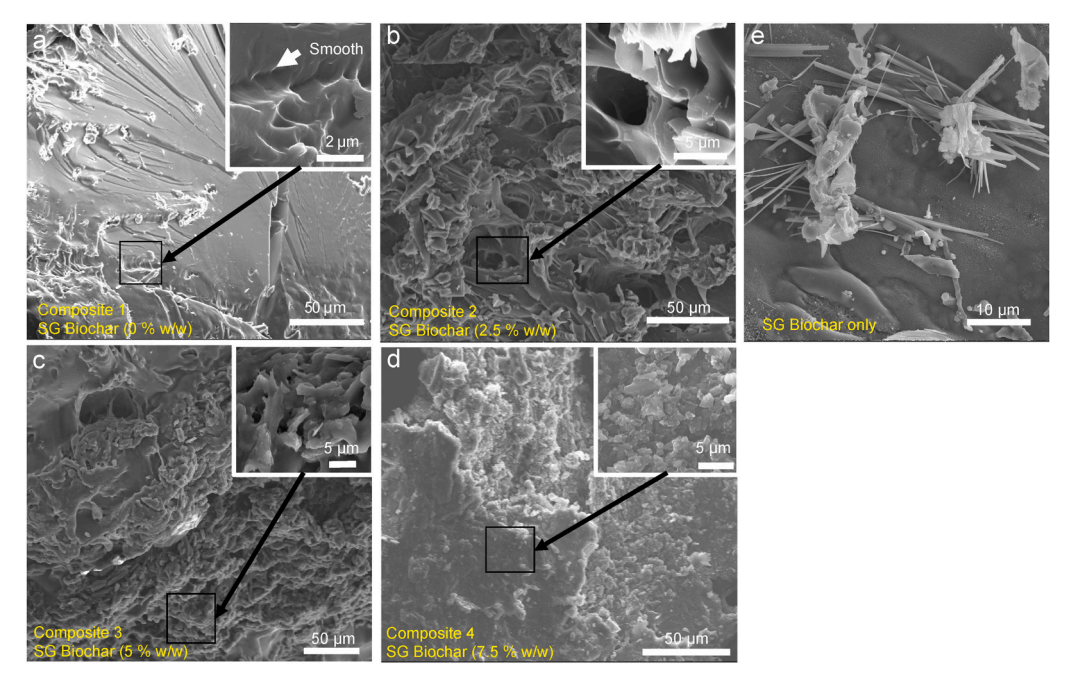


Fig. 3. SEM images of (a) composite 1; (b) composite 2; (c) composite 3; (d) composite 4 and (e) SG biochar.

3.3. Morphology analysis of biochar-hydrogel composites

A well-defined three-dimensional interconnected porous surface allows the transportation of guest molecules such as water and nitrogen to diffusion and/or release [32]. Thus, the microstructure of composite is an important component to study. The composite without biochar (composite 1) has a compact surface structure (Fig. 3 (a)). This indicate the homogenous distribution of raw materials after the microwave-irradiated synthesis. But the composites with biochar exhibited coarse surfaces, demonstrating biochar dispersed on the matrix surface as well as in the porous structure (Fig. 3 (b)–(d)). Similar observation was reported that a fertilizer-polymer composite (includes chitosan, acrylic acid, bentonite and NH4⁺-loaded biochar) displayed an undulant and coarse surface, resulting from the graft polymerization of raw materials [7]. Irregular bulges dispersing on the surface of composite are positively correlated with the biochar content as reported in literatures [33].

3.4. Water absorbency of biochar-hydrogel composite

Water absorbency capacities had the order of composite 4 > composite 3 > composite 1 > composite 2. Water absorbency capacity has been enhanced by the increasing dosage of biochar (Fig. 4). The differences became more pronounced after 15 h (Fig. 4(b)). However, water absorption rate of composite 2 is slightly slower than the composite without biochar (i.e., composite 1). Comparing to other three composites, only composite 1 showed a decreasing trend after 35 h. It proves that biochar-hydrogel composite has better water swelling capacity and longer water retention ability. The Gallagher-Corrigan model fitted water absorbency of 4 composites (Table 1, R² from 0.9182 to 0.9736). This fitting revealed the two-phase water absorbency profile of four composites: an initial quick burst (phase I) and a polymer relaxation-controlled phase (phase II). During phase I, 77% of water can easily diffused into the polymer matrix. The polymer matrix relaxation is clearly observed after 24 h (phase II), coupling with the nitrogen release behavior. This result is consistent with FTIR results. The transmittance on composite 2 is lower than the composite 1 in the region of 3500 to 3200 cm⁻¹ (Fig. 2 (c)), indicating less hydrophilic C–H and O–H groups on composite 2 than 1. Small amount of biochar on the composite surface might combine with the surface functional group, whereas excessive biochar in composites inversely provides more hydrophilic groups.

3.5. Nitrogen release behavior of biochar-hydrogel composite

Nitrogen release behaviors were significantly different between composites with/without biochar (Fig. 5). Without biochar, the release rate was very slow, which is not sufficient for plant growth. With biochar, nitrogen was steadily released. As discussed above, there was no obvious crosslinking between biochar and other materials in the biochar-hydrogel composite (Fig. 1). Therefore, biochar tied with urea in the composite is likely to be gradually released during the composite expansion (corresponding to phase II of water absorbency profile). Except composite 1, the nutrient release behavior of other 3 composites are all defined as anomalous transport, indicating a combination of diffusion and polymer relaxation [23]. Composite 1 is defined as a case II transport (n = 1.1507), which is independent to time. The nutrient release from composite 1 is controlled by matrix relaxation (Table 2).

Indicated from the results, hydrogel-biochar composites with these advanced characteristics could effectively improve the utilization of nutrients and water. When imbedded in the soil, the composites are able to release nutrients along with portion of biochar, enhancing soil moisture content simultaneously. Indicating from previous studies, nitrogen released from the composite not only require sufficient amount, but also on-time amount according to the needs of plants. For example, snap bean has a slothful nutrient uptake (~10% of total nitrogen) at first 30 days followed by a rapid uptake (~40% of total nitrogen) lasting for a month [34]. A slower rate at the beginning and a following rapid release is optimal for plants' need. Anomalous transport of composite 2 to 4 indicated that polymer matrix relaxation gradually occurred during the nutrient release (Table 2). Therefore, nitrogen release is expected to constantly increase afterwards, which fits the plants' need (Fig. 5).

3.6. Cost benefit evaluation of microwave-irradiated polymerization method

Production cost (per ton of composite) of hydrogel-biochar composite is various due to the different local prices of raw materials, energy

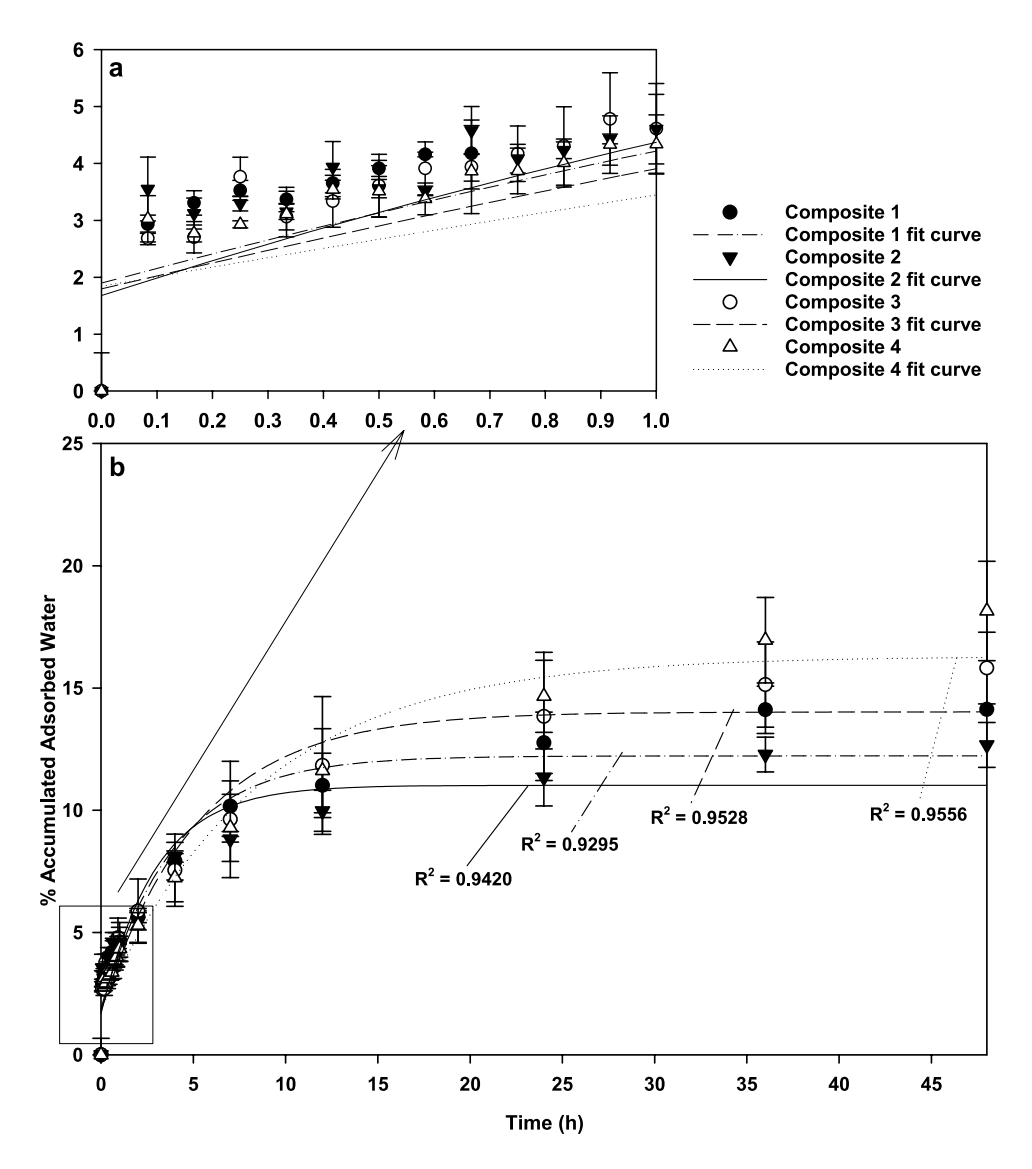


Fig. 4. Water absorbency capacity (%) of hydrogel-biochar composite (p < 0.01) (a) in first 1 h and (b) in 45 h.

Table 1Kinetic fitting parameters of water absorbency of hydrogel-biochar composite.

Composite #	Gallagher-Corrigan Model					
	(Mt/ M∞) _B	(Mt/ M∞) _{max}	$k_{g,1}$	$k_{g,2}$	R ²	
Composite 1	10.40	13.37	$\begin{array}{c} 3.87 \times \\ 10^{-3} \end{array}$	3.22×10^{-12}	0.9420	
Composite 2	9.42	12.27	6.05×10^{-3}	3.24×10^{-12}	0.9295	
Composite 3	12.25	15.97	3.06×10^{-3}	3.25×10^{-12}	0.9528	
Composite 4	14.94	19.40	$1.60\times\\10^{-3}$	$^{1.26\times}_{10^{-14}}$	0.9556	

input, and labor cost. But the comparison of lab-scale polymerization methods could be realized. For example, polyacrylamide polymerization required different experimental conditions in radical polymerization with microwave heating and conventional heating. The amount of initiator, crosslinker and solvent are largely reduced during the microwave polymerization (Table 3). In addition, it has been estimated that microwave irradiation yield reaction rate enhancement of about 130–150% comparing to conventional methods [35]. Therefore,

assuming the same protocol was applied to the pretreatments (homogenous stir, degassing, pH adjustment), the microwave irradiation can reduce at least 40% of the cost than conventional polymerization. The scale-up microwave reaction (size > 1 L) is relatively hard to be estimated because limited information [36]. But there are several successful pilot-scaled examples (1000 t/year) provided by Microwave Chemical Co. showing the promising applications (food additives, polyester, nanoparticle etc.) of this technology. Hydrogel and biochar are all desirable soil amendments but without large scale utilization. High demand and lack of production contributed to the high pricing of these soil amendments [11]. With the utilization of microwave-irradiated polymerization, it is believed that production efficiency can be enhanced, and manufacturing cost can be largely reduced.

4. Conclusions

The result showed that microwave irradiation was successfully employed to polymer composite production. Short time period (i.e., 2-min duration) and clean production process were the dominant advantages observed during the synthesis. After the synthesis, microwave-mediated biochar-hydrogel composite exhibited appreciate water retention and prolonged nutrient releasing capacity. Estimating from the

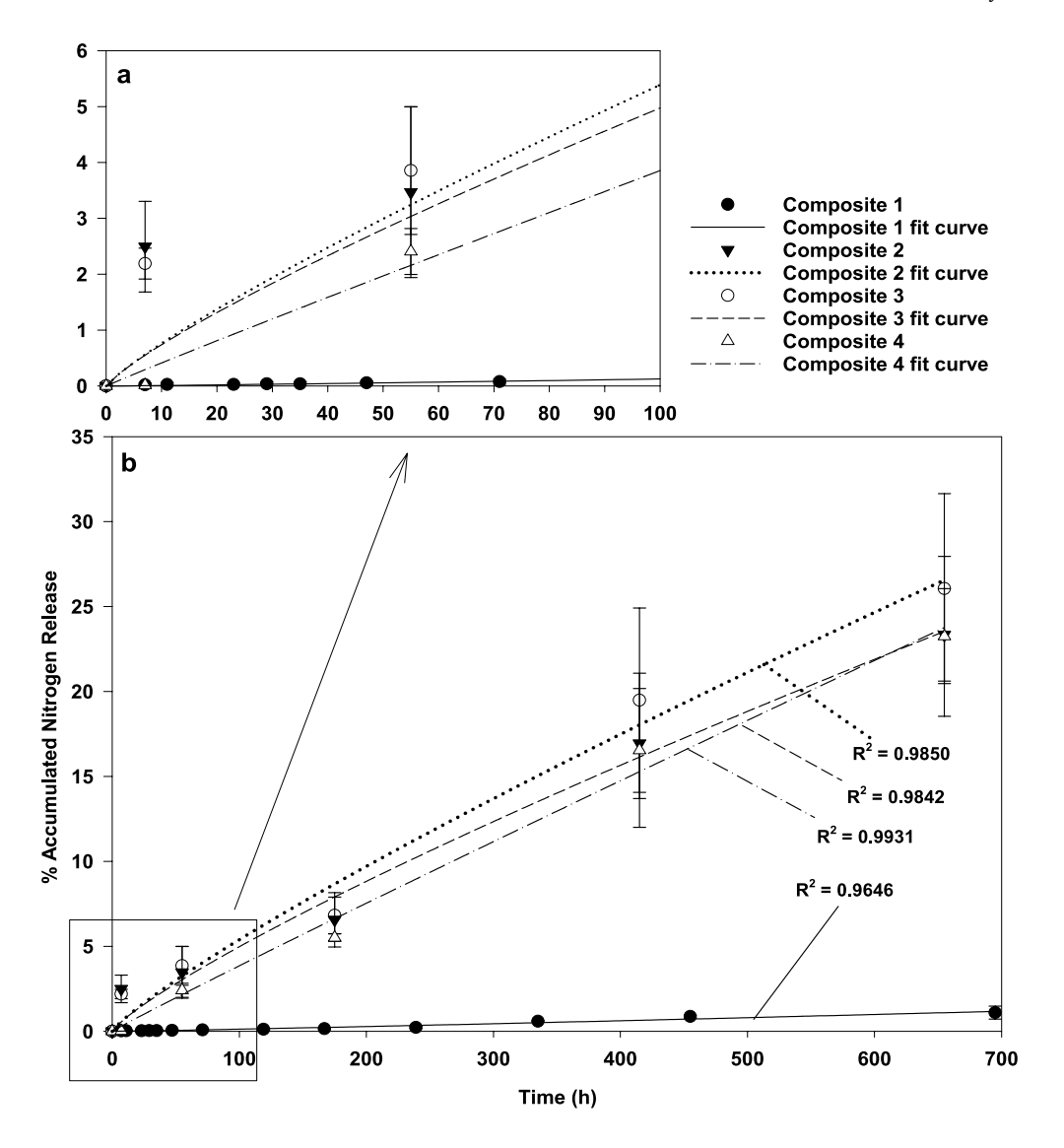


Fig. 5. Accumulated nitrogen release (%) of hydrogel-biochar composite (p < 0.01) (a) in first 100 h and (b) in 700 h.

Table 2Kinetic fitting parameters of nitrogen release from hydrogel-biochar composite.

Composite #	Korsmeyer-Peppas Model			Transport Mechanism
	K_k	n	R^2	
Composite 1	$6.28 \times 10^{-4} \\ 0.1106$	1.1507	0.9646	Case II transport
Composite 2		0.8266	0.9850	Anomalous transport
Composite 3	0.1230	0.8485	0.9842	Anomalous transport
Composite 4	0.0447	0.9677	0.9931	Anomalous transport

scanning electron microscope (SEM), biochar dispersed uniformly in the porous matrix and onto the polymer surface. Thermogravimetric analysis (TGA) indicated the thermal stability of linkages between cellulose and acrylamide, but not with the biochar. FT-IR analysis demonstrated the major functional groups of biochar-hydrogel composites. The linkages between cellulose and acrylamide were believed to maintain the polymer matrix where biochar can be attached on and a reservoir to store significant amount of water. The study revealed the significant role of biochar in the hydrogel composite. It enhanced the moisture retention as well as liberated nitrogen in an appropriate amount according to plants' need. Based on the cost benefit analysis and literature survey, it is expected that microwave-assisted products will circumvent disadvantages with conventional products.

Table 3Experimental conditions in polymerizations with microwave and with conventional heating.

	Microwave irradiation	Dosage	Conventional heating	Dosage
Initiator	Potassium Persulfate, Ammonium Persulfate	5% (w/w total raw materials)	Potassium Persulfate	0.8% (w/w total raw materials)
Crosslinker	N, <i>N</i> - bisacrylamide Methylene	1–5% (w/w total raw materials)	N, <i>N</i> - bisacrylamide Methylene	0.8% (w/w total raw materials)
Solvent	Sodium Hydroxide, Urea, Distilled Water	1 g products/ 2.5 mL	Distilled Water	1 g products/ 2.5 mL
Reaction time Temperature	2 h–20 h 40 °C–70 °C		2 min-15 min 300 W-1200	
or Power level	[10.07.00]		W	01
Reference	[12,37,38] This study [39,40],			

CRediT authorship contribution statement

Yudi Wu: Investigation, Data curation, Visualization, Software, Writing - original draft. **Colten Brickler:** Investigation, Data curation, Software, Writing - review & editing. **Simeng Li:** Conceptualization, Methodology, Validation, Supervision. **Gang Chen:** Supervision, Funding acquisition.

Declaration of competing interest

The authors declare that they have no known competing financial interests or personal relationships that could have appeared to influence the work reported in this paper.

Acknowledgements

The authors acknowledge the support from the National Institute of Food and Agriculture through Grant No. 2018-68002-27920 to Florida A&M University and also the National Science Foundation through Grant No. 1735235 awarded as part of the National Science Foundation Research Traineeship.

References

- [1] T.S. Du, S.Z. Kang, J.H. Zhang, W.J. Davies, Deficit irrigation and sustainable water-resource strategies in agriculture for China's food security, J. Exp. Bot. 66 (8) (2015) 2253–2269, https://doi.org/10.1093/ixb/erv034.
- [2] D. Laird, P. Fleming, B. Wang, R. Horton, D. Karlen, Biochar impact on nutrient leaching from a Midwestern agricultural soil, Geoderma 158 (3–4) (2010) 436–442. http://doi:10.1016/j.geoderma.2010.05.012.
- [3] J.N. Houser, W.B. Richardson, Nitrogen and phosphorus in the Upper Mississippi River: transport, processing, and effects on the river ecosystem, Hydrobiologia 640 (1) (2010) 71–88, https://doi.org/10.1007/s10750-009-0067-4.
- [4] Y.P. Timilsena, R. Adhikari, P. Casey, T. Muster, H. Gill, B. Adhikari, Enhanced efficiency fertilisers: a review of formulation and nutrient release patterns, J. Sci. Food Agric. 95 (6) (2015) 1131–1142. https://doi.org/10.1002/jsfa.6812.
- [5] X. Gao, C. Li, M. Zhang, R. Wang, B. Chen, Controlled release urea improved the nitrogen use efficiency, yield and quality of potato (Solanum tuberosum L.) on silt loamy soil, Field Crop. Res. 181 (2015) 60–68, https://doi.org/10.1016/j. fcr.2015.07.009.
- [6] C. Scheer, D.W. Rowlings, M. De Antoni Migliorati, D.W. Lester, M.J. Bell, P. R. Grace, Effect of enhanced efficiency fertilisers on nitrous oxide emissions in a sub-tropical cereal cropping system, Soil Res. 54 (5) (2016) 544–551, https://doi.org/10.1071/SR15332.
- [7] P. Wen, Z.S. Wu, Y.J. Han, G. Cravotto, J. Wang, B.C. Ye, Microwave-assisted synthesis of a novel biochar-based slow-release nitrogen fertilizer with enhanced water-retention capacity, ACS Sustain. Chem. Eng. 5 (8) (2017) 7374–7382, https://doi.org/10.1021/acssuschemen.7b01721.
- [8] S. Jeffery, D. Abalos, M. Prodana, A.C. Bastos, J.W. Van Groenigen, B.A. Hungate, F. Verheijen, Biochar boosts tropical but not temperate crop yields, Environ. Res. Lett. 12 (5) (2017), 053001, https://doi.org/10.1088/1748-9326/aa67bd.
- [9] C. Liang, X. Zhu, S. Fu, A. Méndez, G. Gascó, J. Paz-Ferreiro, Biochar alters the resistance and resilience to drought in a tropical soil, Environ. Res. Lett. 9 (6) (2014), 064013, https://doi.org/10.1088/1748-9326/9/6/064013.
- [10] S. Chen, M. Yang, C. Ba, S. Yu, Y. Jiang, H. Zou, Y. Zhang, Preparation and characterization of slow-release fertilizer encapsulated by biochar-based waterborne copolymers, Sci. Total Environ. 615 (2018) 431–437, https://doi.org/ 10.1016/j.scitotenv.2017.09.209.
- [11] S. Li, G. Chen, Contemporary strategies for enhancing nitrogen retention and mitigating nitrous oxide emission in agricultural soils: present and future, Environ. Dev. Sustain. 22 (4) (2020) 2703–2741, https://doi.org/10.1007/s10668-019-00327-2
- [12] S. Kim, G. Iyer, A. Nadarajah, J.M. Frantz, A.L. Spongberg, Polyacrylamide hydrogel properties for horticultural applications, Int. J. Polym. Anal. Char. 15 (5) (2010) 307–318, https://doi.org/10.1080/1023666X.2010.493271.
- [13] M. Curcio, N. Picci, Polymer in agriculture: a review, Am. J. Agric. Biol. Sci. 3 (1) (2008) 299–314, https://doi.org/10.3844/ajabssp.2008.299.314.
- [14] S. Mohammadi-Khoo, P.N. Moghadam, A.R. Fareghi, N. Movagharnezhad, Synthesis of a cellulose-based hydrogel network: characterization and study of urea fertilizer slow release, J. Appl. Polym. Sci 133 (5) (2016), https://doi.org/ 10.1002/app.42935.
- [15] C.J. Clarke, W.-C. Tu, O. Levers, A. Brohl, J.P. Hallett, Green and sustainable solvents in chemical processes, Chem. Rev. 118 (2) (2018) 747–800, https://doi. org/10.1021/acs.chemrev.7b00571.
- [16] I. Kyrikou, D. Briassoulis, Biodegradation of agricultural plastic films: a critical review, J. Polym. Environ. 15 (2) (2007) 125–150, https://doi.org/10.1007/ s10924-007-0053-8.

- [17] K. Pang, R. Kotek, A. Tonelli, Review of conventional and novel polymerization processes for polyesters, Prog. Polym. Sci. 31 (11) (2006) 1009–1037, https://doi. org/10.1016/j.progpolymsci.2006.08.008.
- [18] S.S. Lam, E. Azwar, W.X. Peng, Y.F. Tsang, N.L. Ma, Z.L. Liu, Y.K. Park, E.E. Kwon, Cleaner conversion of bamboo into carbon fibre with favourable physicochemical and capacitive properties via microwave pyrolysis combining with solvent extraction and chemical impregnation, J. Clean. Prod. 236 (2019), https://doi.org/ 10.1016/j.jclepro.2019.117692.
- [19] G. Giachi, M. Frediani, L. Rosi, P. Frediani, Synthesis and processing of biodegradable and bio-based polymers by microwave irradiation, in: U. Chandra (Ed.), Microwave Heating, 2011, pp. 181–206.
- [20] M. Pandey, N. Mohamad, M.C.I.M. Amin, Bacterial cellulose/acrylamide pH-sensitive smart hydrogel: development, characterization, and toxicity studies in ICR mice model, Mol. Pharm. 11 (10) (2014) 3596–3608, https://doi.org/10.1021/mp500337r
- [21] S. Li, G. Chen, Thermogravimetric, thermochemical, and infrared spectral characterization of feedstocks and biochar derived at different pyrolysis temperatures, Waste Manag. 78 (2018) 198–207, https://doi.org/10.1016/j. wasman.2018.05.048.
- [22] C. Chang, L. Zhang, Cellulose-based hydrogels: present status and application prospects, Carbohydr. Polym. 84 (1) (2011) 40–53, https://doi.org/10.1016/j. carbool.2010.12.023.
- [23] J. Siepmann, N.a.A. Peppas, Modeling of drug release from delivery systems based on hydroxypropyl methylcellulose (HPMC), Adv. Drug Deliv. Rev. 64 (2012) 163–174, https://doi.org/10.1016/S0169-409X(01)00112-0.
- [24] R. Ullah, S.U.D. Khan, M. Aamir, R. Ullah, Terahertz time domain, Raman and fourier transform infrared spectroscopy of acrylamide, and the application of density functional theory, J Spectrosc (Hindawi) 2013 (2013), https://doi.org/ 10.1155/2013/148903.
- [25] M.Z. Afzal, X.-F. Sun, J. Liu, C. Song, S.-G. Wang, A. Javed, Enhancement of ciprofloxacin sorption on chitosan/biochar hydrogel beads, Sci. Total Environ. 639 (2018) 560–569, https://doi.org/10.1016/j.scitotenv.2018.05.129.
- [26] K. Varaprasad, T. Jayaramudu, R. Sadiku, Removal of dye by carboxymethyl cellulose, acrylamide and graphene oxide via a free radical polymerization process, Carbohydr. Polym. 164 (2017) 186–194, https://doi.org/10.1016/j. carbool 2017 01 094
- [27] X. Liu, J. Liao, H. Song, Y. Yang, C. Guan, Z. Zhang, A biochar-based route for environmentally friendly controlled release of nitrogen: urea-loaded biochar and bentonite composite, Sci. Rep. 9 (1) (2019) 9548, https://doi.org/10.1038/ s41598-019-46065-3.
- [28] A.J.M. Valente, A.J.F.N. Sobral, A. Jiménez, S. Patachia, A.R.C.B. Oliveira, V.M. M. Lobo, Effect of different electrolytes on the swelling properties of calyx[4] pyrrole-containing polyacrylamide membranes, Eur. Polym. J. 42 (9) (2006) 2059–2068, https://doi.org/10.1016/j.eurpolymj.2006.04.002.
- [29] C. Zhou, Q. Wu, A novel polyacrylamide nanocomposite hydrogel reinforced with natural chitosan nanofibers, Colloids Surf., B 84 (1) (2011) 155–162, https://doi. org/10.1016/j.colsurfb.2010.12.030.
- [30] Y. Bao, J. Ma, N. Li, Synthesis and swelling behaviors of sodium carboxymethyl cellulose-g-poly(AA-co-AM-co-AMPS)/MMT superabsorbent hydrogel, Carbohydr. Polym. 84 (1) (2011) 76–82, https://doi.org/10.1016/j.carbpol.2010.10.061.
- [31] S. Sethi, B.S. Kaith, Saruchi, V. Kumar, Fabrication and characterization of microwave assisted carboxymethyl cellulose-gelatin silver nanoparticles imbibed hydrogel: its evaluation as dye degradation, React. Funct. Polym. 142 (2019) 134–146, https://doi.org/10.1016/j.reactfunctpolym.2019.06.014.
- [32] C.B. Godiya, X. Cheng, D. Li, Z. Chen, X. Lu, Carboxymethyl cellulose/ polyacrylamide composite hydrogel for cascaded treatment/reuse of heavy metal ions in wastewater, J. Hazard Mater. 364 (2019) 28–38, https://doi.org/10.1016/ j.jhazmat.2018.09.076.
- [33] W. Zhang, J. Song, Q. He, H. Wang, W. Lyu, H. Feng, W. Xiong, W. Guo, J. Wu, L. Chen, Novel pectin based composite hydrogel derived from grapefruit peel for enhanced Cu(II) removal, J. Hazard Mater. 384 (2020) 121445, https://doi.org/ 10.1016/j.jhazmat.2019.121445.
- [34] G. Liu, L. Zotarelli, Y. Li, D. Dinkins, Q. Wang, M. Ozores-Hampton, in: F.C. E. Service (Ed.), Controlled-release and Slow-Release Fertilizers as Nutrient Management Tools, Hortic. Sci. Dep, 2014.
- [35] D. Bogdal, 4.39 microwave-assisted polymerization, in: K. Matyjaszewski, M. Möller (Eds.), Polymer Science: A Comprehensive Reference, Elsevier, Amsterdam, 2012, pp. 981–1027.
- [36] J.D. Moseley, P. Lenden, M. Lockwood, K. Ruda, J.-P. Sherlock, A.D. Thomson, J. P. Gilday, A comparison of commercial microwave reactors for scale-up within process chemistry, Org. Process Res. Dev. 12 (1) (2008) 30–40, https://doi.org/10.1021/op700186z.
- [37] S.K. Ghazali, N. Adrus, J. Jamaluddin, Pineapple leaf fibers coated with polyacrylamide hydrogel, Appl. Mech. Mater. 695 (2015) 139–142. http://doi.org/10.4028/www.scientific.net/AMM.695.139.
- [38] E.M. Ahmed, Hydrogel: Preparation, characterization, and applications: a review, J. Adv. Res. 6 (2) (2015) 105–121, https://doi.org/10.1016/j.jare.2013.07.006.
- [39] R. Nagahata, K. Takeuchi, Encouragements for the use of microwaves in industrial chemistry, Chem. Rec. 19 (1) (2019) 51–64, https://doi.org/10.1002/ tcr.201800064.
- [40] R. Hoogenboom, R.M. Paulus, Å. Pilotti, U.S. Schubert, Scale-up of microwave-assisted polymerizations in batch mode: the cationic ring-opening polymerization of 2-Ethyl-2-oxazoline, Macromol. Rapid Commun. 27 (18) (2006) 1556–1560, https://doi.org/10.1002/marc.200600349.